Vol. **114** (2008) *ACTA PHYSICA POLONICA A* No. 2

Proceedings of the 7-th National Meeting of Synchrotron Radiation Users

XANES Studies of Mn K and $L_{3,2}$ Edges in the (Ga,Mn)As Layers Modified by High Temperature Annealing

A. Wolska[a,*], K. Lawniczak-Jablonska[a], M.T. Klepka[a], R. Jakieła[a], J. Sadowski[a,b], I.N. Demchenko[a], E. Holub-Krappe[c], A. Persson[d] and D. Arvanitis[d]

[a]Institute of Physics, Polish Academy of Sciences
al. Lotników 32/46, 02-668 Warsaw, Poland
[b]Lund University, MAX-Lab, Lund SE-221 00, Sweden
[c]Hahn–Meitner Institute, Department of Magnetism
Glienicker Str. 100, D-14109 Berlin, Germany
[d]Physics Department, Uppsala University, Box 530, 75121 Uppsala, Sweden

$Ga_{1-x}Mn_xAs$ is commonly considered as a promising material for microelectronic applications utilizing the electron spin. One of the ways that allow increasing the Curie temperature above room temperature is to produce second phase inclusions. In this paper $Ga_{1-x}Mn_xAs$ samples containing precipitations of ferromagnetic MnAs are under consideration. We focus on the atomic and electronic structure around the Mn atoms relating to the cluster formation. The changes in the electronic structure of the Mn, Ga and As atoms in the (Ga,Mn)As layers after high temperature annealing were determined by X-ray absorption near edge spectroscopy. The experimental spectra were compared with the predictions of *ab initio* full multiple scattering theory using the FEFF 8.4 code. The nominal concentration of the Mn atoms in the investigated samples was 6% and 8%. We do not observe changes in the electronic structure of Ga and As introduced by the presence of the Mn atoms. We find, in contrast, considerable changes in the electronic structure around the Mn atoms. Moreover, for the first time it was possible to indicate the preferred interstitial positions of the Mn atoms.

PACS numbers: 78.70.Dm, 75.50.Pp

1. Introduction

Among many, $Ga_{1-x}Mn_xAs$ is commonly considered as a promising material for utilizing the electron spin for microelectronic applications. Most of the studies on this compound were devoted to the uniform ternary alloy which is a diluted

*corresponding author; e-mail: wolska@ifpan.edu.pl

ferromagnetic semiconductor with the highest reported so far Curie temperature being 170 K [1–8]. Moreover, it is fairly easy to obtain $Ga_{1-x}Mn_xAs$ samples containing precipitations of ferromagnetic MnAs [9–11]. These precipitations were usually considered as a major drawback. However, since MnAs is a metallic ferromagnet with the Curie temperature of about 318 K, it is possible to prepare the GaAs:MnAs system in such a way that small ferromagnetic nanoparticles are immersed in the semiconductor host lattice. Such a composite material could be considered as a good semiconductor filled with nanomagnets providing a built-in local magnetic field at room temperature. These magnetic MnAs nanoclusters can be produced from a single-phase $Ga_{1-x}Mn_xAs$ material by the post-growth annealing at temperatures higher than 500°C [8, 11].

In the present paper we study the electronic structure around the different elements in the GaAs layers with magnetic inclusions. We take advantage of X-ray absorption near edge spectroscopy (XANES) which provides information from the bulk of the samples, and therefore is not sensitive to the surface contamination. The K and $L_{3,2}$ edges of Mn as well as L_3 edges of Ga and As were investigated and compared with the prediction of *ab initio* calculations using the code FEFF 8.4.

2. Experiment

The $Ga_{0.94}Mn_{0.06}As$ (named A831) and the $Ga_{0.92}Mn_{0.08}As$ (named A833) layers (0.9 and 1 μm thick, respectively) were grown by molecular beam epitaxy on a semi-insulating GaAs(100) substrate at 230°C in ultra high vacuum. The samples were subsequently divided into three parts. One part was left as such to serve as a reference, the second part of the same sample was annealed at the temperature 500°C ("a") and the third one at 600°C ("b") for 30 min to introduce thermally induced changes in the local structure around Mn atoms. The samples without any heat treatment ("ag": "as-grown"), as well as hexagonal MnAs (grown on the (111) and (100) GaAs substrates) were used as the reference samples.

The X-ray absorption measurements at the K edge of Mn were performed at Hasylab (A1 station) using a 7-element Ge fluorescence detector [12]. The L edges of Mn, As and Ga were collected in the total electron yield (TEY) mode at MAX-lab (beamline D-1011). Since the TEY technique, particularly for low excitation photon energies, is more surface sensitive than the fluorescence mode, the samples were sputtered *in situ* in order to remove a thin oxidic layer from the surface. To estimate the content of Mn atoms and check the influence of annealing on the distribution of Mn atoms in the layers, the secondary ion mass spectroscopy (SIMS) measurements using a CAMECA IMS6F micro-analyzer were also carried out.

3. Results and discussion

3.1. SIMS results

SIMS measurements were performed with an oxygen (O_2^+) primary beam, with the current kept at 600 nA. The size of the eroded crater was about

150 μm $\times$ 150 μm and the secondary ions were collected from the central region of 60 μm in diameter. The Mn content was derived from the intensity of the Mn^+ species and the matrix signal, As^+, was taken as a reference. Mn implanted GaAs was used as a calibration standard. The thickness of the examined layer was measured by an Alpha-Step Profiler. The relative error of the Mn content determination in the SIMS method is $\pm 10\%$.

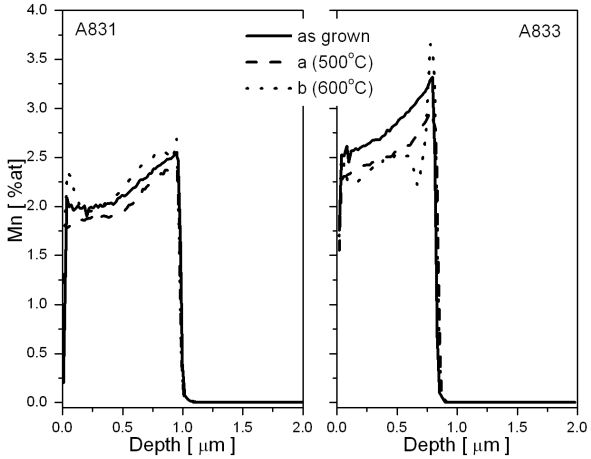

Fig. 1. SIMS depth profiles of the Mn distribution along the growth direction in the as grown and annealed GaMnAs layers.

Results of the SIMS measurements are shown in Fig. 1. The concentration of Mn (x) in all of the examined samples did not change significantly during the annealing but some tendency of an increase at the interface with the GaAs substrate was observed. The content of Mn was at the level: 2–2.5% $\pm$ 0.2 for the A831 series and 2.5–3% $\pm$ 0.3 for the A833 series. It is around 3 times less than the nominal concentration.

3.2. Mn K edge

XANES spectra of the A831 and A833 series as well as the MnAs reference layers are shown in Fig. 2. The differences between respective samples ("ag", "a" and "b") from each set are negligible, an observation which suggests that the Mn atoms have the same local atomic environment for both series. This is not surprising considering the results of the SIMS analysis, which show that samples differ in composition only by 0.5 at% of Mn instead of the nominal 2 at%. However, there is a noticeable change in the shapes of the maxima of the as grown samples in respect of the annealed ones. In the as grown samples we expect to have a $Ga_{1-x}Mn_xAs$ uniform alloy in the layer. The annealing is supposed to introduce the precipitations of the MnAs in the "a" and "b" samples. Comparing the XANES spectra of these samples with the MnAs spectrum, it can be concluded that indeed

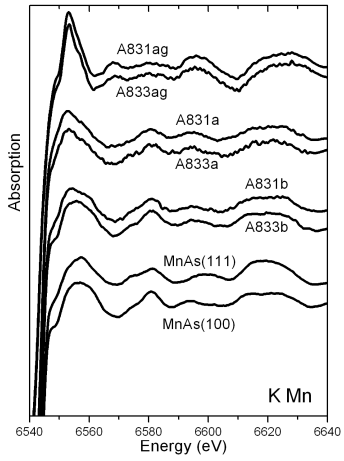

Fig. 2. XANES measurements at the K edge of Mn of the investigated Ga–Mn–As compounds as well as MnAs reference samples.

the local atomic environment of the Mn atoms in annealed samples is similar to those in the MnAs layers.

In order to check how the location of the Mn atoms in the GaAs matrix influences the shape of the XANES the *ab initio* calculations using FEFF 8.4 [13] were carried out. In all cases the procedure we followed was similar. A cluster of 10 Å in radius was first created using the known crystallographic data for MnAs and GaAs structures [14] and then the XANES spectra were calculated using the subsequent cards: XANES, SCF (self-consistent potential calculations) and FMS (full multiple scattering XANES calculations). The Hedin–Lundqvist potential was chosen. The obtained spectra were additionally convolved with a Gaussian function modeling the experimentally induced broadening. In the case of the K edge of Mn the used value of that broadening was equal to 0.5 eV.

Figure 3 shows the result of the calculations compared with the as grown sample represented by A831ag. In the case of this sample, one has to consider different Mn positions in the GaAs matrix: substitutional Mn_{Ga}, interstitial (I) — with As atoms as the first neighbors, interstitial (II) — with Ga atoms as the first neighbors. The FEFF 8.4 calculations of Mn spectra for all these possibilities are shown in Fig. 3. It is clear that none of the theoretical spectra is really close to the experimental one and it is impossible to choose one over another [15]. This fact suggests that Mn atoms may occupy more than one position in the crystal lattice, a fact which is in agreement with the observations that there is usually several percent of Mn atoms that do not subsitute Ga atoms [16–18]. Judging from the shape of the calculated and measured spectra the superposition of Mn_{Ga} and interstitial (II) has a chance to produce the spectrum similar to the experimental one, since in the theoretical interstitial (II) spectrum a pre-peak appears just below the first main maximum, which does not exist in the other models.

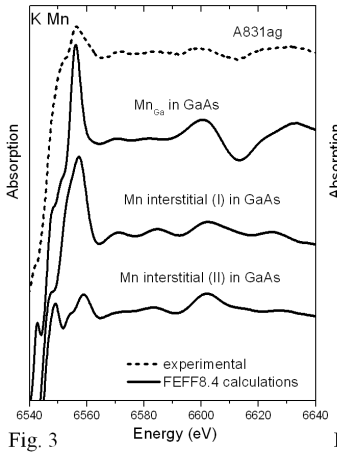

Fig. 3

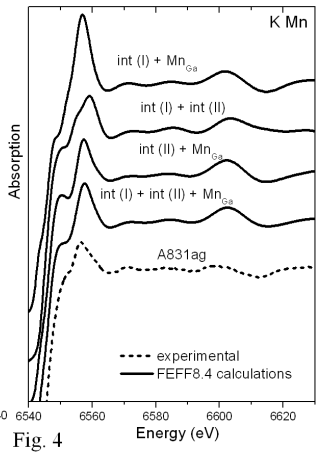

Fig. 4

Fig. 3. Experimental spectrum of A831ag versus FEFF 8.4 calculations for different Mn positions in the GaAs matrix: substitutional Mn_{Ga}, interstitial (I) — As atoms as the first neighbors, interstitial (II) — Ga atoms as the first neighbors.

Fig. 4. Experimental spectrum of A831ag compared with results of different fittings of FEFF 8.4 reference spectra.

In order to check this presumption, the feature called "the linear combination fitting" in the IFEFFIT analysis package: the Athena software [19] was employed. The experimental spectrum was taken as the "unknown" one and the calculated ones as the "reference". Several combinations of the models were considered:

a) interstitial (I) and Mn_{Ga},
b) interstitial (I) and interstitial (II),
c) interstitial (II) and Mn_{Ga},
d) interstitial (I), interstitial (II) and Mn_{Ga}.

TABLE

Results of fitting of Mn K edge reference FEFF 8.4 spectra to the K edge of A831ag experimental one.

	Mn_{Ga} [%]	Interstitial (I) [%]	Interstitial (II) [%]	Reduced χ^2
model (a)	44±5	56±5	–	0.00162
model (b)	–	45±3	55±3	0.00098
model (c)	43±2	–	57±2	0.00076
model (d)	33±3	17±4	50±3	0.00071

The results of the fitting are shown in Fig. 4 and Table. The best fits were obtained in the case of models (c) and (d). This suggests that Mn atoms prefer to be located in the substitutional positions and the interstitial (II). However, it

cannot be excluded that a small part of them are located in the interstitial (I) position.

3.3. Ga and As L_3 edges

The L_3 edges of Ga and As show no differences between the "as grown" and the annealed samples. This observation is understandable because of the low Mn concentration. In order to check how the presence of the Mn atoms can affect the absorption spectra theoretical calculations were performed. Again, experimental broadening was added, with a convolution width equal to 0.4 eV.

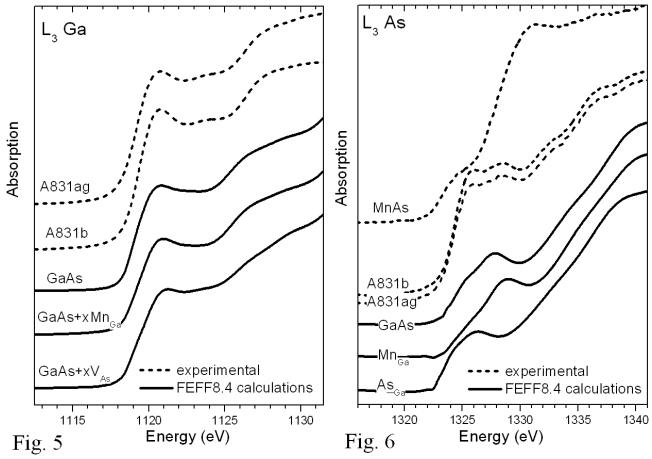

Fig. 5 Fig. 6

Fig. 5. Experimental XANES spectra of Ga L_3 edge compared with FEFF 8.4 calculations of: pure GaAs, GaAs with substitutional Mn (GaAs+xMn$_{\mathrm{Ga}}$) and GaAs with introduced As vacancies (GaAs+xV$_{\mathrm{As}}$).

Fig. 6. Experimental XANES spectra of As L_3 edge compared with FEFF 8.4 calculations of: pure GaAs, GaAs with substitutional Mn (GaAs+xMn$_{\mathrm{Ga}}$) and Ga$_{\mathrm{As}}$ with introduced AsGa antisite defects (GaAs+xAs$_{\mathrm{Ga}}$) as well as MnAs experimental spectrum.

There were several models considered during the calculations, some of which are showed in Figs. 5 and 6. The first — basic — model consists of the ideal GaAs structure. In the second one, few Mn$_{\mathrm{Ga}}$ atoms were introduced in the cluster used for the modeling. In the third model the GaAs layer was modified by adding As vacancies in the cluster. The results of the calculations together with the experimental data are shown in Fig. 5 (L_3 Ga). As can be seen in the plots, the shape of the Ga L_3 edge can be reproduced only by taking into account the V$_{\mathrm{As}}$ contribution. The substitutional Mn$_{\mathrm{Ga}}$ atoms do not affect the theoretical XANES spectrum too much. In the case of the As L_3 edge (Fig. 6), none of the described models is very close to the experimental spectrum. However, the model with the As$_{\mathrm{Ga}}$ antisite defects modifies the theoretical spectrum by shifting the

first maximum energy to the same energy as for the first maximum in the experimental spectrum. This observation suggests that this type of defects exists in the GaAs matrix. Unfortunately, it was not possible to perform a fitting as described previously in Athena because the corresponding feature of the program does not work well for L_3 edges. A comparison of data A831ag and the MnAs spectra (Fig. 6) excluded the possibility of the presence of MnAs inclusions (observed in the annealed samples) in a significant amount that would influence the shape of the As edge. Retrospectively, this seems to be obvious knowing that Mn in the sample is present in the amount of 2 at%.

3.4. Mn $L_{3,2}$ edges

XANES spectra of Mn $L_{3,2}$ edges for both series and MnAs are shown in Fig. 7. The shapes of the spectra look rather similar. However, upon more precise inspection, we observe that the edges of the as grown samples are shifted towards lower energy (around 0.2 eV) in respect of the annealed ones. The rather sharp

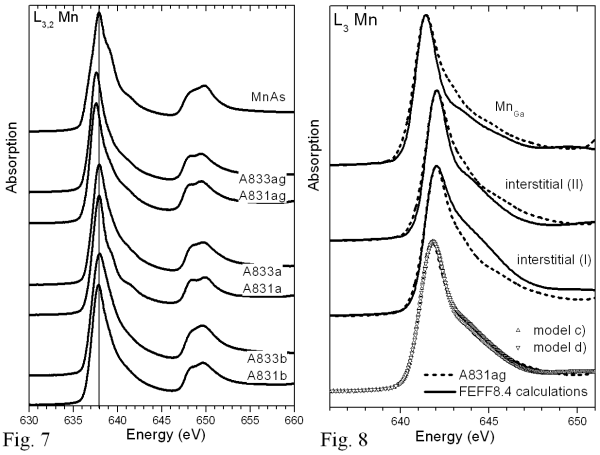

Fig. 7

Fig. 8

Fig. 7. Experimental XANES spectra of Mn $L_{3,2}$ edges for A831 and A833 series and MnAs.

Fig. 8. XANES spectrum of A831ag Mn L_3 edge compared with FEFF8.4 calculations for different Mn positions in the GaAs matrix: substitutional Mn_{Ga}, interstitial (I) — As atoms as the first neighbors, interstitial (II) — Ga atoms as the first neighbors and FEFF8.4 calculations of MnAs.

and intensive $L_{3,2}$ white lines superimposed to the atomic double step continuum at the $L_{3,2}$ edges are due to transitions to final states with d-symmetry. These are much more localized than the s-symmetry states projected in the K edge. Therefore the influence of the long-range order on the spectrum shape is expected to be, in principle, much less pronounced.

The Mn L_3 spectra for the annealed samples appear to be close to that of MnAs in shape and edge position. This is another confirmation of the existence

of MnAs inclusions. A more complicated situation was observed in the K edge of the as grown samples. Therefore, these spectra were taken under closer examination and the FEFF 8.4 calculations were performed in the way described in Sect. 3.2. The experimental broadening was added by convolution with the Gaussian function with width equal to 0.4 eV.

An important detail that one should be aware of during the calculations is that in case of L edges, the FEFF 8.4 code very often does not give the right energy position of the edge. This is why in the comparisons with the experiment the full width at half maximum was taken under consideration and not the energy position of the edge. Figure 8 shows a comparison between the spectrum of the as grown sample and the FEFF 8.4 calculations for the models described in the Mn K edge case: substitutional Mn_{Ga}, interstitial (I) — As atoms as the first neighbors and interstitial (II) — Ga atoms as the first neighbors. The theoretical spectra were left in the energies given by the program. In order to compare them, the XANES spectrum of the A831ag sample was shifted to match the energy position with the calculated spectra.

It can be seen that the spectrum for the Mn_{Ga} and interstitial (II) models are close to the experimental one. There is substantial difference in the results for the interstitial (I) model where the full width at half maximum is significantly wider than for other models. From these results, it can be concluded that the interstitial Mn atoms prefer a position with Ga atoms as the first neighbors (interstitial II). The weighted sum of the theoretical L_3 spectra performed with the values obtained from Mn K edge fitting shows good agreement for (c) and (d) models as in the previous case (Fig. 8).

4. Conclusions

The XANES measurements of the K edge of Mn proved that the local structure of Mn atoms in the annealed samples is close to the hexagonal MnAs references and remarkably differ from the "as grown" sample.

The comparison of the K and $L_{3,2}$ spectra of the as grown sample with the FEFF 8.4 calculations which assumed different position of Mn atoms in the GaAs matrix and fitting the reference theoretical spectra to the experimental one, helped to determine possible Mn atom positions in the matrix and their relative percentage. It appears that more than 50% of the Mn atoms is found in the interstitial position with the Ga atoms as the nearest neighbors but one cannot exclude that few percent of Mn atoms may have the As atoms as nearest neighbors. The percentage of interstitial Mn atoms is found higher than is usually expected. This is due to the fact that the samples were examined as grown without low temperature annealing which is usually performed to populate the substitutional position with Mn atoms. The performed analysis for the first time indicates which interstitial position for Mn atoms is more probable.

The L_3 edges of Ga and As show no differences between the "as grown" and annealed samples. That is understandable because of the low Mn concentration.

However, in the case of the Ga L_3 edge, a comparison with FEFF 8.4 calculations shows that As vacancies were introduced, an observation typical of low temperature grown GaMnAs samples [20]. In the case of the As L_3 edge, the calculations show that As_{Ga} antisite defects have to be taken under consideration.

Acknowledgments

This work was partially supported by national grant of the Ministry of Science and High Education (Poland) N202-052-32/1189 as well as by DESY/HASYLAB, MAX-lab (EC support program: Transnational Access to Research Infrastructures) and the European Community under contract RII3-CT-2004-506008 (IA-SFS).

References

[1] H. Ohno, F. Matsukura, *Solid State Commun.* **117**, 179 (2001).

[2] J.L. Xu, M. van Schilfgaarde, G.D. Samolyuk, *Phys. Rev. Lett.* **94**, 097201 (2005).

[3] Y.L. Soo, G. Kioseoglou, S. Kim, X. Chen, H. Luo, Y.H. Kao, Y. Sasaki, X. Liu, J.K. Furdyna, *Appl. Phys. Lett.* **80**, 2654 (2002).

[4] Y.L. Soo, G. Kioseoglou, S. Kim, X. Chen, H. Luo, Y.H. Kao, H.-J. Lin, H.H. Hsieh, T.Y. Hou, C.T. Chen, Y. Sasaki, X. Liu, J.K. Furdyna, *Phys. Rev. B* **67**, 214401 (2003).

[5] Y.L. Soo, S. Wang, S. Kim, G. Kim, M. Cheon, X. Chen, H. Luo, Y.H. Kao, Y. Sasaki, X. Liu, J.K. Furdyna, *Appl. Phys. Lett.* **83**, 2354 (2003).

[6] F. d'Acapito, G. Smolentsev, F. Boscherini, M. Piccin, G. Bais, S. Rubini, F. Martelli, A. Franciosi, *Phys. Rev. B* **73**, 035314 (2006).

[7] R. Shioda, K. Ando, T. Hayashi, M. Tanaka, *Phys. Rev. B* **58**, 1100 (1998).

[8] M. Adell, L. Ilver, J. Kanski, V. Stanciu, P. Svedlindh, J. Sadowski, J.Z. Domagala, F. Terki, C. Hernandez, S. Charar, *Appl. Phys. Lett.* **86**, 112501 (2005).

[9] H. Ohno, *J. Magn. Magn. Mater.* **200**, 110 (1999).

[10] H. Shimuzu, M. Miyamura, M. Tanaka, *J. Vac. Sci. Technol. B* **18**, 2063 (2000).

[11] I.N. Demchenko, K. Lawniczak-Jablonska, T. Story, V. Osinniy, R. Jakiela, J.Z. Domagala, J. Sadowski, M. Klepka, A. Wolska, *Phys. Condens. Matter* **19**, 496205 (2007).

[12] http://hasylab.desy.de/facilities/doris_iii/beamlines/a1/experimental_station/detectors/7_pixel_hpge_detector/index_eng.html.

[13] A.L. Ankudinov, B. Ravel, J.J. Rehr, S.D. Conradson, *Phys. Rev. B* **58**, 7565 (1998).

[14] R.W.G. Wyckoff, *Crystal Structures*, Vol. 1, 2nd ed., Interscience Publ., New York 1963, p. 85.

[15] R. Bacewicz, A. Twarog, A. Malinowska, T. Wojtowicz, X. Liu, J.K. Furdyna, *J. Phys. Chem. Solids* **66**, 2004 (2005).

[16] K.M. Yu, W. Walukiewicz, T. Wojtowicz, I. Kuryliszyn, X. Liu, Y. Sasaki, J.K. Furdyna, *Phys. Rev. B* **65**, 201303R (2002).

[17] J. Masek, J. Kudrnovsky, F. Maca, *Phys. Rev. B* **67**, 153203 (2003).

[18] I. Kuryliszyn-Kudelska, J.Z. Domagala, T. Wojtowicz, X. Liu, E. Lusakowska, W. Dobrowolski, J.K. Furdyna, *J. Appl. Phys.* **95**, 603 (2004).

[19] B. Ravel, M. Newville, *J. Synchrotron Rad.* **12**, 537 (2005).

[20] J.N. Gleason, M.E. Hjelmstad, V.D. Dasika, R.S. Goldman, S. Fathpour, S. Charkrabarti, P.K. Bhattacharya, *Appl. Phys. Lett.* **86**, 011911 (2005).